RSC Advances

PAPER

View Article Online
View Journal | View Issue

Cite this: *RSC Adv.*, 2024, **14**, 21544

Furan and benzene ring formation in cellulose char: the roles of 5-HMF and reducing ends†

Takashi Nomoura, Eiji Minami and Haruo Kawamoto*

The authors previously proposed that 5-hydroxymethylfurfural (5-HMF) can be produced from the reducing ends of cellulose as a key intermediate during carbonization. The present work investigated the mechanisms by which furan and benzene rings are formed in cellulose char based on carbonization at 280 °C using ^{13}C-labeled 5-HMF together with ^{13}C-labeled glucose (as a model for the cellulose reducing ends). Glycerol was added to the 5-HMF to prevent the formation of stable glassy polymers. The resulting char was subjected to pyrolysis gas chromatography/mass spectrometry (764 °C, 5 s hold time) and the incorporation of ^{13}C in furan-, phenol-, benzofuran- and benzene-type fragments was assessed. The apparent formation mechanisms include a direct rearrangement of the six carbons of 5-HMF to phenols, Diels–Alder reactions of furan rings with double bonds to give benzofurans and a more random process involving reactive fragments producing benzene rings. On the basis of these results, the roles of 5-HMF and reducing ends during cellulose carbonization are discussed herein.

Received 7th May 2024
Accepted 27th June 2024

DOI: 10.1039/d4ra03344b

rsc.li/rsc-advances

Introduction

Pyrolysis including carbonization is a potential means of producing biochar, biofuels and biochemicals from lignocellulosic biomass. The utilization of these pyrolysis-based products is expected to play a key role in mitigating global warming by reducing overall anthropogenic CO_2 emissions to the atmosphere. In particular, the addition of biochar to soils has recently received attention as an approach to removing atmospheric CO_2 to achieve the 2050 carbon neutrality target.[1] However, it is important to both understand and control pyrolysis reactions to develop efficient pyrolysis-based conversion technologies.

The initial process in the thermal decomposition of cellulose is a decrease in the degree of polymerization (DP) of the material.[2–5] As an example, the DP of Whatman cellulose has been reported to decrease from 2650 to 200–400 following heating to temperatures in the range of 175–225 °C.[4] Subsequent to this, both dehydration and carbonization reactions occur. Based on the van Krevelen diagram for this process, which plots the H/C ratio against the O/C ratio in the cellulose char, Tang and Bacon found that dehydration was the primary reaction occurring during the carbonization of cellulose in the range of 200–280 °C.[6] The dehydration of Whatman cellulose was found to take place between 200 and 350 °C, with a total mass-based water yield of 14.3%.[7]

As carbonization progresses, benzene rings are formed in the cellulose char,[8–12] as confirmed by the generation of benzene carboxylic acids following alkaline permanganate oxidation.[10] This formation of aromatic groups in the char has also been confirmed by pyrolysis gas chromatography/mass spectrometry (Py-GC/MS) and ^{13}C nuclear magnetic resonance (NMR) spectroscopy.[8–11]

Pastorova *et al.*[9] characterized cellulose char using both Py-GC/MS and ^{13}C-NMR spectroscopy and reported that the chemical structure transitioned from cellulose through a furan-based structure to a benzene-based structure as carbonization progressed. Both furfural and 5-hydroxymethylfurfural (5-HMF) have been proposed as the intermediate compounds formed during the hydrothermal treatment of reducing sugars.[13] Because water is produced from the reducing ends of cellulose during carbonization in conjunction with the formation of 5-HMF, conditions similar to those applied during hydrothermal treatment could be created within cell walls composed of cellulose.[3] In fact, it has been reported that oligosaccharides, which are products of cellulose hydrolysis, are formed from cellulose during pyrolysis.[14]

Characteristic infrared (IR) bands at 1600 and 1700 cm^{-1} appear early in the carbonization of cellulose and are assigned to conjugated double bonds and carbonyl (C=O) groups.[6,8,9,15] These peaks are believed to result from dehydration reactions. It has also been reported that the treatment of cellulose with glycerol or $NaBH_4$, which eliminates the reducing ends of the material, greatly suppresses thermal discoloration and carbonization.[3,5,16] These findings indicate that the reducing ends of cellulose play an important role in carbonization.

Graduate School of Energy Science, Kyoto University, Yoshida-honmachi, Sakyo-ku, Kyoto 606-8501, Japan. E-mail: kawamoto.haruo.2m@kyoto-u.ac.jp

† Electronic supplementary information (ESI) available. See DOI: https://doi.org/10.1039/d4ra03344b

Aprotic solvents, such as certain aromatic compounds, have been found to stabilize primary cellulose pyrolysis products, including levoglucosan and 5-HMF, by acting as hydrogen acceptors.[17,18] The authors recently reported that the formation of solid carbonized products (meaning black, non-hydrolysable substances) was inhibited during trials in aromatic solvents whereas 5-HMF was evidently generated.[18] As an example, the yield of solid char from the carbonization of cellulose (Whatman no. 42 filter paper) at 280 °C was decreased from 50.7 wt% under N_2 to nil when performed in benzophenone, while the yield of 5-HMF increased from 0.0 wt% (under N_2) to 6.4 wt%. In addition, the char obtained from the carbonization of 5-HMF and glycerol (a model of coexisting primary products from cellulose pyrolysis) was confirmed to provide similar pyrograms to those of cellulose containing various benzene- and benzofuran-type fragments.[19] Phenolic and carboxylic acid groups were also detected in both types of char. Based on these results, it appears that 5-HMF may be a key intermediate in cellulose carbonization.[19]

Despite the findings noted above, the mechanism by which furan and benzene rings are formed from 5-HMF and the reducing ends during cellulose carbonization is still not clearly understood. In the present study, these processes were therefore investigated using ^{13}C-labeled 5-HMF and ^{13}C-labeled glucose, with the latter serving as a model for the reducing ends of cellulose.

Results and discussion

Py-GC/MS analysis of ^{13}C-labeled glucose

Unlabeled glucose and three different types of ^{13}C-labeled glucose (1-^{13}C-, 2-^{13}C- and 6-^{13}C-labeled) were subjected to Py-GC/MS analysis using a Curie point injector at 280 °C with a hold time of 15 s under a He flow. Fig. 1 shows the pyrogram obtained from the unlabeled glucose. These data exhibit two large signals assigned to 5-HMF and furfural, indicating that the glucose produced these compounds upon pyrolysis.

The mass spectra of 5-HMF and furfural generated from trials using unlabeled and ^{13}C-labeled glucose samples are presented in Fig. 2. The molecular ion (M^+) of the unlabeled 5-HMF (originally at *m*/*z* of 126) was shifted to *m*/*z* of 127 in the spectra generated from the three ^{13}C-labeled glucose samples.

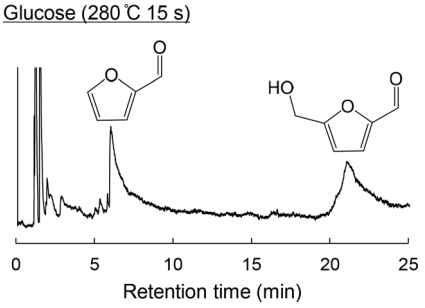

Fig. 1 Pyrogram obtained from the Py-GC/MS analysis of unlabeled glucose (280 °C, 15 s hold time).

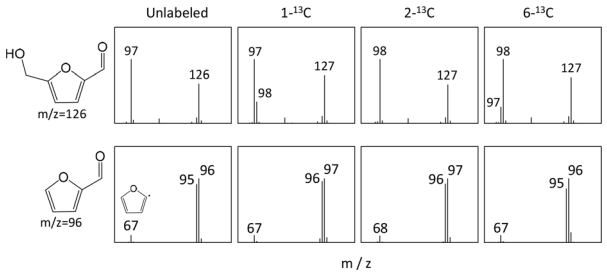

Fig. 2 Mass spectra of 5-HMF and furfural produced from the pyrolysis of unlabeled and labeled glucose.

This shift demonstrated that the six carbons of the glucose were directly rearranged to produce 5-HMF.

The fragment ion of 5-HMF at *m*/*z* of 97 generated by the unlabeled glucose is attributed to the elimination of the aldehyde group (CHO, *m*/*z* 29) from 5-HMF, providing insights into the process by which the glucose was converted to 5-HMF. The fragment from the 2-^{13}C-labeled glucose appeared at *m*/*z* of 98, indicating that the isotopically labeled carbon had been incorporated into the furan ring. The mass spectra acquired from the 1-^{13}C- and 6-^{13}C-labeled glucose samples were more complex and both contained *m*/*z* 97 and 98 fragments but with different intensities. The significantly higher intensity of the *m*/*z* 98 peak generated by the 6-^{13}C-labeled glucose confirms that the carbon in the aldehyde group of the 5-HMF was primarily derived from the 1-C carbon of the glucose, whereas the hydroxymethyl group was derived from the 6-C site of the glucose.[20] The 1-^{13}C-labeled glucose provided the same results.

In experiments with 2-^{13}C-labeled glucose, the fragment ion of furfural at *m*/*z* of 67, formed by the removal of the aldehyde group, was shifted to *m*/*z* of 68. This result shows that 2-C of the glucose has been incorporated into the furan ring. These data also suggest that the aldehyde group originated from the 1-C carbon of the glucose.[20–22]

The two most prominent ions in the spectrum of the furfural (M^+ at *m*/*z* of 96 and M^+-1 at *m*/*z* of 95) from the unlabeled glucose appeared at *m*/*z* of 97 and 96 in experiments with 1-^{13}C- and 2-^{13}C-labeled glucose, respectively, but not in experiments with 6-^{13}C-labeled glucose. These data indicate that the 6-C site of glucose was removed during the pyrolytic production of furfural from glucose. There has been controversy as to whether furfural is produced from 5-HMF or directly from glucose.[22,23] In the present study, 6-C of glucose was specifically removed during furfural formation, whereas the incorporation of 1-C of glucose into the aldehyde carbon of 5-HMF was less selective and some 6-C of glucose was also converted into the aldehyde group of 5-HMF. These results suggest that furfural was not formed *via* 5-HMF during the pyrolysis of glucose at 280 °C.

Based on the present results and on literature information,[20–24] a heterolytic mechanism for the formation of 5-HMF and furfural from glucose is shown in Fig. 3. This process is initiated by the dehydration reaction *via* a six-membered transition state involving an enol intermediate formed by keto–enol tautomerization.[20,24] Whether 5-HMF or furfural is formed is determined by whether reaction (1) or (2)

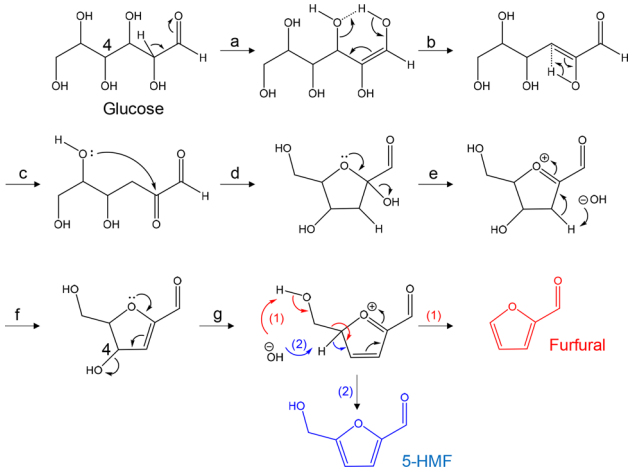

Fig. 3 Pathways for the pyrolytic conversion of glucose to 5-HMF and furfural.

occurs to generate the furan ring from the oxonium intermediate, as proposed by Paine *et al.*[22] This mechanism can explain the formation of furfural from glucose without *via* 5-HMF.

These pathways also suggest that a reducing sugar is required for the dehydration to 5-HMF and furfural to proceed. Since the glycosidic bond is cleaved in the dehydration step (step g), the reducing ends of cellulose would be expected to undergo the same sequence of reactions as in a peeling reaction.

Py-GC/MS analysis of char obtained from ^{13}C-labeled 5-HMF and ^{13}C-labeled glucose

Either 2-^{13}C-, 6-^{13}C- or 7-^{13}C-labeled 5-HMF (5 mg) prepared from 2-^{13}C-, 1-^{13}C- or 6-^{13}C-labeled glucose (Fig. 4) was carbonized in the presence of glycerol (40 mg), serving as a model for pyrolysis products of cellulose, at 280 °C for 60 min under N_2. As demonstrated in our previous work,[19] pure 5-HMF tends to form hard glassy polymers when heated to 280 °C and these materials are resistant to subsequent carbonization. This unwanted homopolymerization was suppressed by the addition of glycerol. It should be noted that thermal degradation products other than 5-HMF are also generated during actual cellulose carbonization. The 1-^{13}C-, 2-^{13}C- and 6-^{13}C-labeled glucose samples (5 mg) were also heated under similar conditions but no glycerol was used.

The resulting char fractions were analyzed by Py-GC/MS at 764 °C with a hold time of 5 s under a He flow. The char was pyrolyzed to release volatile fragments and the structures and ^{13}C incorporation patterns of these fragments provided insights

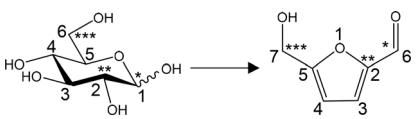

Fig. 4 Production of 5-HMF from glucose and numbering of the carbon atoms.

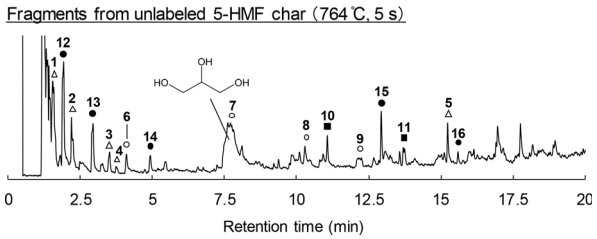

Fig. 5 Pyrogram obtained from the Py-GC/MS analysis (764 °C, 5 s hold time) of 5-HMF char generated by carbonization at 280 °C for 60 min.

into the composition and formation mechanism of the original char. Fig. 5 shows the pyrogram for the char fraction obtained from unlabeled 5-HMF, while the molecular structures of the identified signals are summarized in Fig. 6. In this pyrogram, the phenol (7) signal overlaps with the glycerol used for pyrolysis. The pyrogram acquired from unlabeled glucose char, shown in Fig. S1,† was found to be similar and the ^{13}C-labeled glucose samples also generated essentially equivalent data.

Prior work by the authors[19,25] demonstrated that furan-, benzofuran-, phenol- and benzene-type fragments could be identified by the Py-GC/MS analysis of 5-HMF char, which produced pyrograms similar to those obtained from cellulose char (data not shown here). Therefore, these structures were evidently present as components of the char produced from 5-HMF, glucose and cellulose.

Fig. 7 provides the mass spectra of the volatile fragments generated from the unlabeled and labeled 5-HMF char specimens. The mass spectra obtained from unlabeled and ^{13}C-labeled glucose char samples are shown in Fig. S2.† The proportions of unlabeled products and those incorporating one,

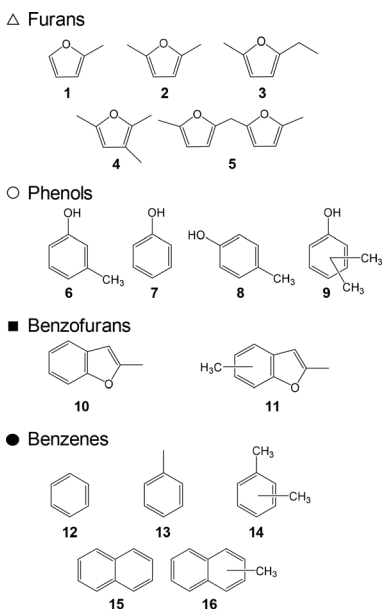

Fig. 6 Molecular structures of the volatile fragments identified by Py-GC/MS analysis (764 °C, 5 s hold time) of 5-HMF char obtained by carbonization at 280 °C for 60 min.

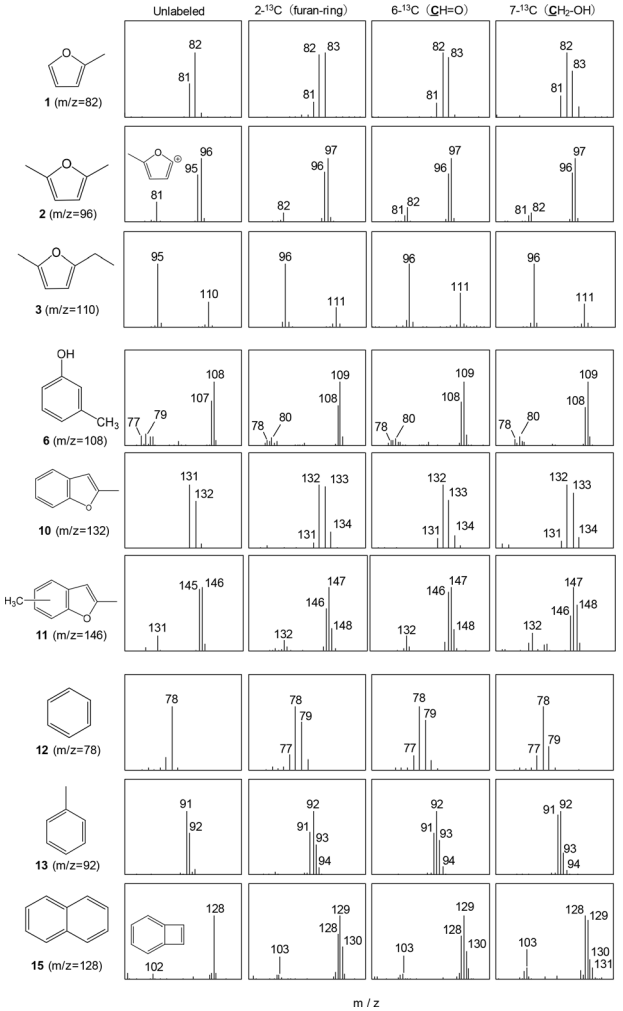

Fig. 7 Mass spectra of volatile fragments generated by Py-GC/MS analysis (764 °C, 5 s hold time) of unlabeled and labeled 5-HMF chars obtained by carbonization at 280 °C for 60 min.

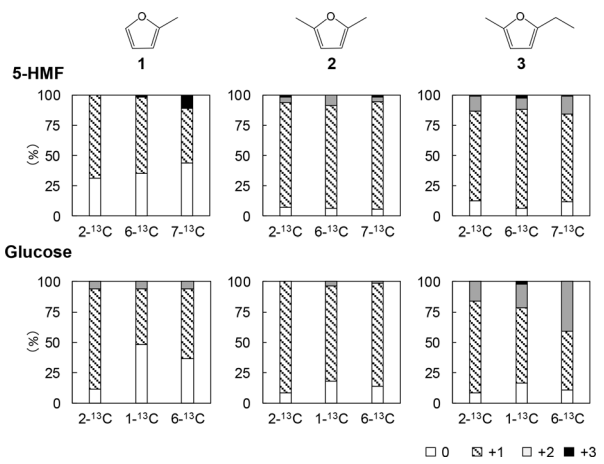

Fig. 8 Proportions of furan-type fragments generated by Py-GC/MS analysis (764 °C, 5 s hold time) of the char fractions prepared from ^{13}C-labeled 5-HMF and ^{13}C-labeled glucose samples (280 °C, 60 min) containing ^{13}C atoms at various sites and in various quantities.

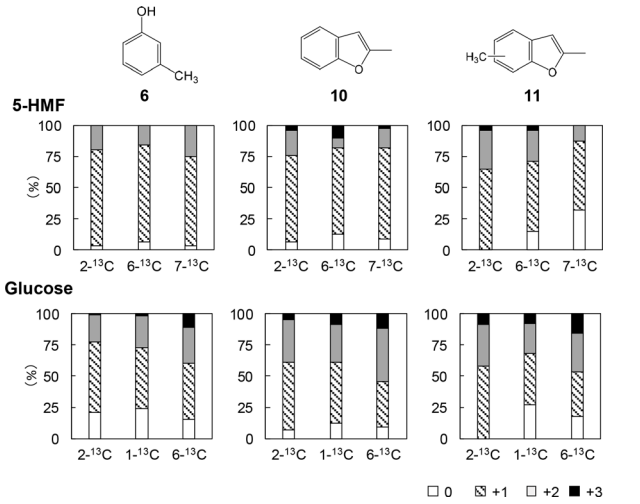

Fig. 9 Proportions of phenol- and benzofuran-type fragments generated by Py-GC/MS analysis (764 °C, 5 s hold time) of the char fractions prepared from ^{13}C-labeled 5-HMF and ^{13}C-labeled glucose samples (280 °C, 60 min) containing ^{13}C atoms at various sites and in various quantities.

two or three ^{13}C atoms can be ascertained by comparing the intensity of the M^+ peak to those of nearby peaks. Fig. 8–10 summarize the proportions of furan, phenol/benzofuran and benzene type products containing ^{13}C atoms at various sites and in various quantities. Note that different carbon numbering systems were used for the glucose and 5-HMF (Fig. 4). Comparing the results obtained from the experiments with glucose and 5-HMF provides information concerning the pyrolytic degradation of the reducing ends of cellulose and the roles of 5-HMF and furfural during cellulose carbonization. It should also be noted that, in the case of the ^{13}C-labeled 5-HMF, a large amount of unlabeled glycerol was added to the pyrolysis medium, thus diluting the ^{13}C concentration as glycerol carbons are incorporated into the 5-HMF.

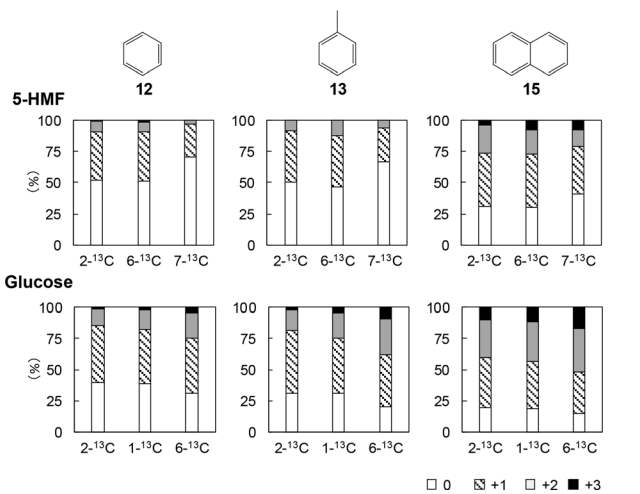

Fig. 10 Proportions of benzene-type fragments generated by Py-GC/MS analysis (764 °C, 5 s hold time) of the char fractions prepared from ^{13}C-labeled 5-HMF and ^{13}C-labeled glucose samples (280 °C, 60 min) containing ^{13}C atoms at various sites and in various quantities.

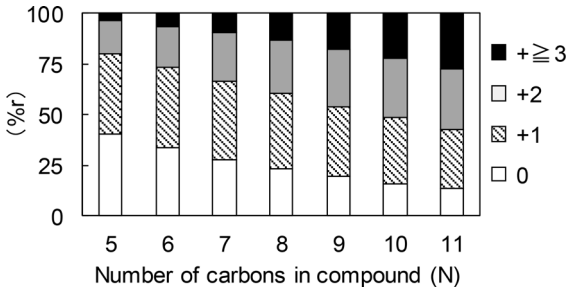

Fig. 11 The %*r* values calculated for those fragments with carbon numbers 5–11 generated during Py-GC/MS analyses. These data assume that the carbons of ^{13}C-labeled 5-HMF and ^{13}C-labeled glucose were randomly distributed in the fragments.

In the case of the ^{13}C-labeled glucose samples, the percentage of ^{13}C stochastically distributed in the volatile fragments (*via* some random mechanism) is referred to herein as %*r* (+*n*), where *n* is a numeral from 1 to 3 indicating the quantity of ^{13}C atoms in the molecule. This value was calculated as

$$\%r\ (+n) = (1/6)^n \times (N/6)^{N-n} \times {}_N\mathrm{C}_n, \quad (1)$$

where *N* is the number of carbon atoms in the molecule. These %*r* values are summarized in Fig. 11 and Table S1† for *N* from 5 to 11. This range was selected because C5–C11 fragments were identified during the Py-GC/MS analyses. It should be noted that, as discussed above, the ^{13}C proportion in each ^{13}C-labeled 5-HMF product was diluted by unlabeled carbon atoms from the glycerol.

The extent to which ^{13}C atoms were incorporated was found to vary depending on the specific volatile fragment generated during the Py-GC/MS analysis of the char. The results were also not greatly different for the 5-HMF and glucose experiments except for the benzene-type products (Fig. 10). The percentages of benzene (**12**), toluene (**13**) and naphthalene (**15**) containing no ^{13}C were generally higher for the 5-HMF char, indicating that the unlabeled carbons of the glycerol, which was used added for the 5-HMF trials, were incorporated into the char.

Among the furan-type products, dimethylfuran (**2**) and ethylmethylfuran (**3**) had relatively low proportions of molecules containing no ^{13}C (5.5–12.5% when generated from 5-HMF and 8.3–17.6% when generated from glucose). From these data, it appears that fragments **2** and **3** originated from 5-HMF in the condensation products generated with glycerol present in the char fraction. In contrast, the percentage of methylfuran (**1**) containing no ^{13}C obtained from the labeled 5-HMF was relatively high at 31.2–43.5%. These data indicate that significant amounts of the isotopically labeled carbons were removed during carbonization. In particular, the relatively high percentage of methylfuran containing no ^{13}C generated when using the 2-^{13}C-labeled 5-HMF (31.2%) suggests that furan rings were newly constructed in the 5-HMF char, likely by random mechanisms that also provided the benzene-type fragments.

In contrast to the case of 2-^{13}C-labeled 5-HMF, fragment **1** obtained using the 2-^{13}C-labeled glucose showed a low percentage of molecules containing no ^{13}C (11.7%), indicating that pathways not involving 5-HMF are possible for the pyrolysis of glucose. Intermediates in the formation of 5-HMF in Fig. 3 may have generated furan rings in the glucose char.

It should be noted that the percentage of 3-methylphenol (**6**) generated from the 5-HMF char and containing no ^{13}C was quite low (3.1–6.3%, Fig. 9). Hence, this compound must have resulted from the direct rearrangement of the six carbons of 5-HMF into a benzene ring. The ratios of molecules containing two ^{13}C to those containing one were 0.26, 0.21, and 0.36 for trials with the 2-^{13}C-, 6-^{13}C- and 7-^{13}C-labeled 5-HMF char, respectively. Because these ratios were close to the ^{13}C/^{12}C ratio of the ^{13}C-labeled 5-HMF (0.2), the methyl substituent of fragment **6** appears to have been derived from the carbons of 5-HMF. Similar trends were also observed for the phenol (**7**) and dimethylphenol (**9**) (Fig. S3†).

The percentage of 3-methylphenol (**6**) generated using the ^{13}C-labeled glucose sample and containing no ^{13}C was higher at 14.9–24.2% (Fig. 9). These data suggest that pathways other than the direct rearrangement of 5-HMF, likely random mechanisms, also occurred during the glucose carbonization.

A reasonable mechanism for the direct rearrangement of 5-HMF to give a benzene ring in a phenol-type fragment is presented in Fig. 12. This conversion requires ring opening of the furan ring prior to the formation of the benzene ring. In this process, a conjugated oxonium intermediate (formed by elimination of the hydroxymethyl hydroxyl group by electron donation from the ring oxygen) is attacked by water to form a hemiacetal intermediate (reaction b). This intermediate is readily converted to the ring-opening product (reaction c), which is then converted to a cyclohexanedione with a six membered ring *via* an intramolecular aldol condensation (reaction d). This compound is subsequently converted to trihydroxybenzene. Note that the carbon numbering on the molecular structures is based on that shown for 5-HMF to assist in tracking the fate of each carbon atom. The formation of 1,2,4-trihydroxybenzene during the carbonization of cellulose in the

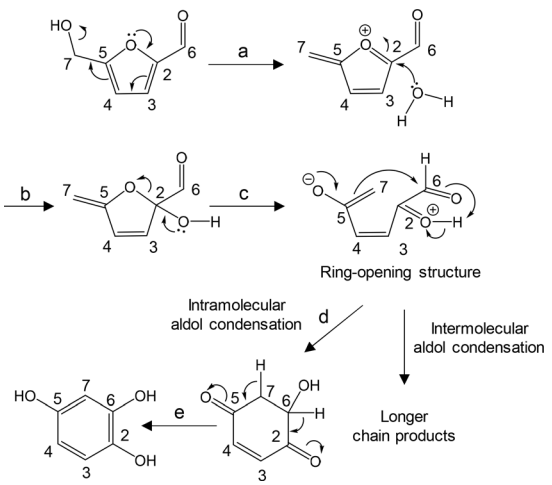

Fig. 12 A proposed mechanism for the conversion of 5-HMF to 1,2,4-trihydroxybenzene. The carbon atom numbering is based on 5-HMF.

presence of sodium chloride was previously observed,[24] although the formation mechanism was not elucidated. Phenols **6**, **7**, **8** and **9** with a single hydroxyl group were detected as volatile fragments by removal of hydroxyl groups during carbonization and Py-GC/MS analysis.

This proposed mechanism is supported by the mass fragment ions at *m*/*z* of 77 and 79 generated in experiments using the unlabeled 5-HMF. These would have resulted from the loss of CO from the C–OH group of 3-methylphenol (**6**) (Fig. 13). In the enlarged spectra, the peaks obtained using the 7-^{13}C-labeled 5-HMF are seen to shift to *m*/*z* of 78 and 80, whereas both pairs of peaks (*m*/*z* 77/79 and 78/80) are observed in the spectra produced using the 2-^{13}C- and 6-^{13}C-labeled 5-HMF. In the mechanism shown in Fig. 12, hydroxyl groups are attached at the C-2 and C-6 positions of the trihydroxybenzene but not at the C-7 site (using the 5-HMF numbering). Thus, the ^{13}C atom of the 7-^{13}C-labeled 5-HMF must remain in **6**, although the ^{13}C atoms at 2-C and 6-C may be lost in the form of ^{13}CO.

Because the intermediates involved in the mechanism shown in Fig. 12 contain carbonyl groups, intra- and intermolecular aldol condensations are possible, as in the case of reaction d. These reactions can generate longer hydrocarbon chains, allowing the formation of additional aromatic rings.

The methylated benzofuran **11** obtained using the 2-^{13}C-labeled 5-HMF and glucose samples contained no detectable molecules having zero ^{13}C atoms, indicating that random mechanisms were not important in the formation of this product. Lower percentages of the 2-^{13}C isomers were also observed in the case of benzofuran **10**. Because the 2-C of glucose was incorporated into the furan ring, this ring would have been involved in the formation of the benzene ring of the benzofuran structure.

Fig. 14 presents a proposed mechanism explaining these results. This mechanism includes the Diels–Alder reaction of the furan ring with a double bond of the ring-opening intermediate shown in Fig. 12. In this pathway, four carbons of the furan ring, including 2-C, are incorporated into the benzene ring, which explains the very low percentage of molecules containing no ^{13}C obtained using the 2-^{13}C-labeled 5-HMF and glucose. The relatively higher percentages of such products generated in trials with the 6-^{13}C- and 7-^{13}C-labeled 5-HMF and

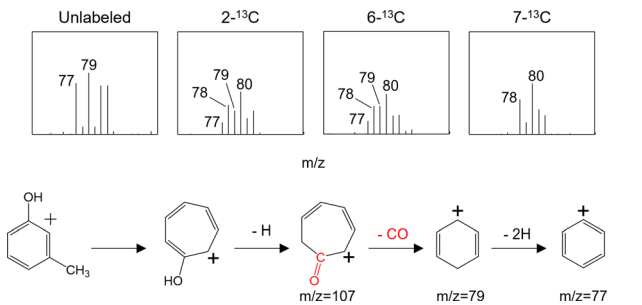

Fig. 13 Enlarged views of the mass spectra of 3-methylphenol (**6**) as obtained from Py-GC/MS analyses of labeled and unlabeled 5-HMF char fractions together with a diagram showing the fragmentation path.

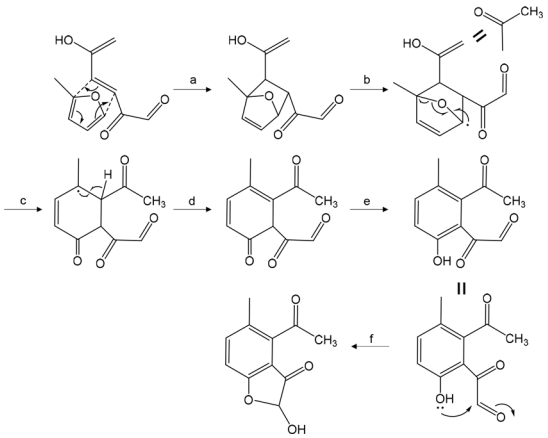

Fig. 14 A possible aromatization pathway *via* the Diels–Alder reaction of a furan ring with the double bond of the ring-opening intermediate obtained from 5-HMF.

glucose can be explained by the possibility of removing the ^{13}C-containing side chains attached to the benzene ring during the Py-GC/MS analysis. A reasonable pathway for the formation of the furan ring of benzofuran can also be devised by including an attack of the phenolic hydroxyl group on the aldehyde carbon.

The compositions of the benzene-type fragments without oxygen substituents were very different from those of the furan-, phenol- and benzofuran-type fragments. The proportions of benzene (**12**), toluene (**13**) and naphthalene (**15**) containing nil, one, two and three ^{13}C atoms obtained from the labeled glucose samples were close to the %*r* values for the corresponding carbon numbers. These results establish that the ^{13}C atoms were randomly incorporated into the aromatic rings of **12**, **13** and **15**. The results obtained using the 2-^{13}C-glucose were similar, and so the Diels–Alder reactions involved in the formation of the benzofurans (Fig. 14) were likely not important for this group of fragments. Rather, benzene rings would have been formed in the char by reactive intermediates produced by the degradation of glucose, including the pathway shown in Fig. 3. Cyclohexyl rings were likely initially generated, as shown in the mechanisms in Fig. 12 and 14, followed by conversion to benzene rings.

It is also noted that the percentages of **12**, **13** and **15** molecules containing no ^{13}C produced using the labeled 5-HMF (29.7–70.6%) were much higher than the corresponding %*r* values as well as the values for the labeled glucose trials. This outcome suggests that the unlabeled carbons of the glycerol used to carbonize the labeled 5-HMF were incorporated into the benzene rings, resulting in dilution of the ^{13}C content, as discussed above.

The mechanisms for the formation of furan-, phenol-, benzofuran- and benzene-type structures in the cellulose char proposed on the basis of the present study using ^{13}C labeling are summarized in Fig. 15.

Role of reducing ends and 5-HMF in cellulose carbonization

The data obtained from this work provide insight into the carbonization of crystalline cellulose. Fig. 16 summarizes the

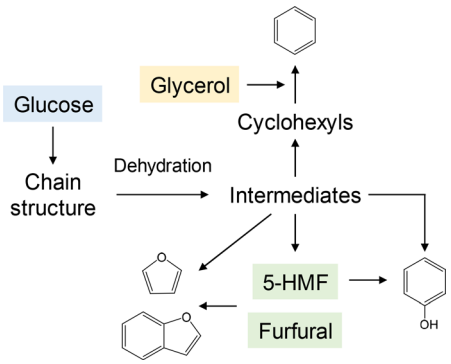

Fig. 15 Summary of the pathways involved in the formation of furan-, phenol-, benzofuran- and benzene-type structures in cellulose char based on the results of the present study.

events occurring during the early stage of cellulose carbonization. Cellulose is more thermally stable than other amorphous polysaccharides because of its crystalline nature. Paracrystalline regions are periodically present in cellulose and the first step in pyrolysis involves a reduction in the degree of polymerization to approximately 200–400 *via* cleavage of glucosidic bonds in these areas to generate new reducing ends.[2–5]

The reducing ends of cellulose are more labile than other repeating units and non-reducing units, as confirmed by the stabilization of cellulose following glycosidation of the reducing ends with alcohols[16] or the reduction to alditol ends with $NaBH_4$.[3,5] Hence, the pyrolytic reactions observed for glucose in the present work are expected to occur for these reducing ends. The reactions of 5-HMF and furfural would also be involved because these compounds were produced from glucose. As discussed above, the 4-C–O–1-C bond (that is, the glucosidic bond) can be cleaved during the dehydration reaction in the mechanism shown in Fig. 3. On this basis, the degradation of the reducing ends can proceed as a kind of "peeling" reaction during which new reducing ends are continually generated.

During thermogravimetric analysis, cellulose tends to exhibit an induction period prior to the initial mass loss. This activation stage has been attributed to the formation of so-called active cellulose, as in the Broido–Shafizadeh kinetic model.[26] Previous work by the authors examined the role of water produced from the reducing ends in this activation process,[3,27] albeit with limited evidence. The results of the present study appear to confirm that 5-HMF, furfural and their formation intermediates (Fig. 3) are key intermediate in cellulose carbonization.

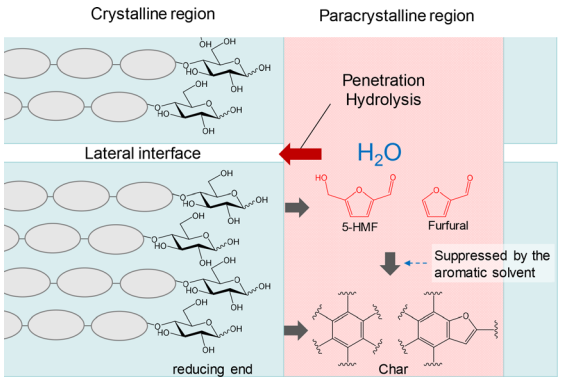

Fig. 16 A diagram showing the proposed role of reducing ends in the early stage of cellulose carbonization.

Dehydration reactions of the reducing ends of cellulose followed by carbonization produce char in the paracrystalline regions, and water generated during this process can hydrolyze cellulose near these regions. This effect could also lead to water penetration between crystallites followed by hydrolysis. In fact, the pyrolysis of cellulose at relatively low temperatures such as 240 °C tends to give oligosaccharides having reducing ends.[3,28] These processes can improve the mobility of surface cellulose molecules, resulting in greater pyrolytic reactivity.

In our previous study,[19] char formation was greatly suppressed while 5-HMF was formed when using aromatic solvents. This outcome can be explained by the inhibition of heterolysis reactions such as those shown in Fig. 12 and 14, especially intermolecular reactions leading to the formation of aromatics. Non-reducing sugars such as 1,6-anhydro-β-D-glucose (levoglucosan) are reported to be stabilized in aromatic solvents based on inhibition of proton transfer through complexation with the solvents *via* CH/π interactions.[17,29]

Conclusions

The mechanism by which benzene rings are formed from 5-HMF and glucose, with the latter used as a model for cellulose reducing ends, was investigated in trials with ^{13}C-labeled 5-HMF and ^{13}C-labeled glucose at 280 °C for 60 min. The following conclusions were reached.

- Glucose was converted to 5-HMF and furfural, with the aldehyde group derived from the 1-C of glucose. The 6-C was selectively lost in the formation of furfural.
- Both 5-HMF and furfural were formed from glucose by dehydration *via* a six-membered transition state.
- Py-GC/MS analyses of 5-HMF and glucose chars revealed that furan-, benzene-, phenol- and benzofuran-type structures were present in the char.
- Mechanisms for the generation of furan, phenol and benzene rings in the char were proposed based on ^{13}C incorporation data.
- The phenol-type fragments generated during the Py-GC/MS analysis of the 5-HMF char were primarily formed by the direct rearrangement of the six carbons. A formation mechanism was developed by considering the ^{13}C incorporation pattern.
- A pathway involving the Diels–Alder reaction of the furan ring with a double bond formed by ring opening of 5-HMF was suggested for the formation of benzofuran structures.
- The benzene- and naphthalene-type fragments, which contained no oxygen, were evidently produced by non-specific pathways involving reactive fragments.
- Based on the present results, the role of reducing ends during cellulose carbonization was elucidated.
- The carbonization mechanisms revealed in the present study provide insight into developing new technologies for selective depolymerization as well as biochar production.

Experimental

Materials

The 5-HMF used in this work (>95.0%, gas chromatography (GC)) was purchased from Tokyo Chemical Industry, Tokyo, Japan, and used after freeze-drying. The D-[1-^{13}C] glucose, D-[2-^{13}C] glucose, D-[6-^{13}C] glucose (>99.8%, high performance liquid chromatography (HPLC)), glycerol (>98.0%, GC) and acetonitrile (>99.0%, GC) employed in the various trials were purchased from Nacalai Tesque, Inc., Kyoto, Japan, and used without purification. Both 1-butyl-3-methylimidazolium chloride (>98.0%, HPLC) and 12-molybdophosphoric acid were purchased from the FUJIFILM Wako Pure Chemical Corp., Osaka, Japan.

A series of ^{13}C-labeled 5-HMF samples was synthesized from the corresponding ^{13}C-labeled glucose according to a literature procedure.[30] In this process, one of the ^{13}C-labeled glucose reagents (180 mg) was added to a mixture of acetonitrile (0.79 g) and 1-butyl-3-methylimidazolium chloride (2.0 g) at 60 °C and stirred until complete dissolution. To this mixture was added 12-molybdophosphoric acid (18 mg) after which the flask was sealed and the reaction was carried out at 120 °C for 3 h. The sample was subsequently cooled after which 2 ml of water was added and the mixture was neutralized by adding 0.0233 mmol of sodium carbonate. The resulting solution was extracted five times using 10 ml of ethyl acetate for each extraction and subsequently dehydrated on a sodium sulfate column. The resulting product was purified by thin layer chromatography using 5% methanol in $CHCl_3$ as the eluent to give the corresponding ^{13}C-labeled 5-HMF.

Carbonization

Quantities of ^{13}C-labeled 5-HMF (5 mg) and glycerol (40 mg) were transferred into a Pyrex glass tube ampoule (inner diameter, 15.0 mm; wall thickness, 1.75 mm; length, 50 mm). The glycerol was added as a model for cellulose pyrolysis products that can inhibit the formation of thermally stable 5-HMF polymers.[19] The air in the ampoule was replaced with nitrogen (99.99%) prior to sealing, after which the ampoule was inserted into a muffle furnace preheated to 280 °C. After heating for 60 min, the ampoule was removed from the furnace and immediately cooled under a flow of air. The resulting pyrolyzate was washed with water and then dried in an oven at 105 °C for 24 h to obtain a char specimen. It should be noted that the authors have confirmed that glycerol alone is stable under the conditions described above.

Py-GC/MS analysis

The char specimens obtained from the 5-HMF samples were analyzed by Py-GC/MS using a portable Curie-point injector (JCI-22, Japan Analytical Industry, Co. Ltd, Tokyo, Japan) coupled with a GC/MS system (GCMS-QP2010 Ultra, Shimadzu Corp., Kyoto, Japan). In each trial, the char was rapidly heated to 764 °C and held at that temperature for 5 s. The GC/MS conditions were as follows: column, Agilent CPSil 8CB (length, 30 m; diameter, 0.25 mm; film thickness, 0.25 μm); injector temperature, 250 °C; split ratio, 1 : 50; column temperature, 50 °C (3 min), 6 °C min^{-1} to 200 °C, 30 °C min^{-1} to 300 °C, 300 °C (5 min); carrier gas, helium; flow rate, 1.0 ml min^{-1}. The signals obtained in the total-ion chromatogram were assigned by comparing the retention times and mass spectra with those of authentic compounds. For comparison, unlabeled and ^{13}C-labeled glucose samples were also analyzed by Py-GC/MS at 280 °C for 15 s.

Data availability

The authors confirm that the data supporting the findings of this study are available within the article and its ESI.†

Author contributions

Conceptualization, data curation, formal analysis, investigation, methodology, visualization, writing-original daft, T. N.; data curation, visualization, writing-review and editing, E. M.; conceptualization, funding acquisition, methodology, project administration, supervision, writing-review and editing, H. K. All authors have read and agreed to the published version of the manuscript.

Conflicts of interest

There are no conflicts to declare.

Acknowledgements

This research was funded by the JST-Mirai Program under grant number JPMJMI20E3. The sponsors had no role in the study design nor in the collection, analysis and interpretation of data, in the writing of the report or in the decision to submit the article for publication. We thank Edanz (**https://jp.edanz.com/ac**) for editing a draft of this manuscript.

References

1 Y. Li, S. Hu, J. Chen, K. Müller, Y. Li, W. Fu, Z. Lin and H. Wang, *J. Soils Sediments*, 2018, **18**, 546–563; K. Weber and P. Quicker, *Fuel*, 2018, **217**, 240–261; A. Tomczyk, Z. Sokolowska and P. Boguta, *Rev. Environ. Sci. Biotechnol.*, 2020, **19**, 191–215; K. Qian, A. Kumar, H. Zhang, D. Bellmer and R. Huhnke, *Renewable Sustainable Energy Rev.*, 2015, **42**, 1055–1064.

2 F. Shafizadeh and A. G. W. Bradbury, *J. Appl. Polym. Sci.*, 1979, **23**, 1431–1442; F. Shimazu and C. Sterling, *J. Food Sci.*, 1966, **31**, 548–551; O. P. Golova and R. G. Krylova, *Dokl. Akad. Nauk SSSR*, 1960, **135**, 1391–1394; Y. Halpern and S. Patai, *Isr. J. Chem.*, 1969, **7**, 673–683; J. Bouchard, G. Garnier, P. Vidal, E. Chornet and R. P. Overend, *Wood Sci. Technol.*, 1990, **24**, 159–169.

3 S. Matsuoka, H. Kawamoto and S. Saka, *J. Anal. Appl. Pyrolysis*, 2014, **106**, 138–146.

4 A. Broido, A. C. Javier-Son, A. C. Ouano and E. M. Barrall II, *J. Appl. Polym. Sci.*, 1973, **17**, 3627–3635.

5 S. Matsuoka, H. Kawamoto and S. Saka, *Polym. Degrad. Stab.*, 2011, **96**, 1242–1247.
6 M. M. Tang and R. Bacon, *Carbon*, 1964, **2**, 211–220.
7 J. Scheirs, G. Camino and W. Tumiatti, *Eur. Polym. J.*, 2001, **37**, 933–942.
8 Y. Sekiguchi, J. S. Frye and F. Shafizadeh, *J. Appl. Polym. Sci.*, 1983, **28**, 3513–3525.
9 I. Pastorova, R. E. Botto, P. W. Arisz and J. J. Boon, *Carbohydr. Res.*, 1994, **262**, 27–47.
10 R. C. Smith and H. C. Howard, *J. Am. Chem. Soc.*, 1937, **59**, 234–236.
11 F. Shafizadeh and Y. Sekiguchi, *Carbon*, 1983, **21**, 511–516; S. Soares, N. Ricardo, S. Jones and F. Heatley, *Eur. Polym. J.*, 2001, **37**, 737–745.
12 Y. Sekiguchi and F. Shafizadeh, *J. Appl. Polym. Sci.*, 1984, **29**, 1267–1286.
13 M. M. Titirici, M. Antonietti and N. Baccile, *Green Chem.*, 2008, **10**, 1204–1212; N. Baccile, G. Laurent, F. Babonneau, F. Fayon, M. M. Titirici and M. Antonietti, *J. Phys. Chem. C*, 2009, **113**, 9644–9654; C. Falco, F. P. Caballero, F. Babonneau, C. Gervais, G. Laurent, M. M. Titirici and N. Baccile, *Langmuir*, 2011, **27**, 14460–14471; I. van Zandvoort, Y. Wang, C. B. Rasrendra, E. R. H. van Eck, P. C. A. Bruijnincx, H. J. Heeres and B. M. Weckhuysen, *ChemSusChem*, 2013, **6**, 1745–1758.
14 Y. Yu, D. Liu and H. Wu, *Energy Fuels*, 2012, **26**, 7331–7339.
15 S. Julien, E. Chornet, P. K. Tiwari and R. P. Overend, *J. Anal. Appl. Pyrolysis*, 1991, **19**, 81–104.
16 S. Matsuoka, H. Kawamoto and S. Saka, *Carbohydr. Res.*, 2011, **346**, 272–279.
17 T. Hosoya, H. Kawamoto and S. Saka, *Carbohydr. Res.*, 2006, **341**, 2293–2297.
18 T. Nomura, H. Kawamoto and S. Saka, *J. Anal. Appl. Pyrolysis*, 2017, **126**, 209–217.
19 T. Nomura, E. Minami and H. Kawamoto, *ChemistryOpen*, 2021, **10**, 610–617.
20 C. P. Locas and V. A. Yaylayan, *J. Agric. Food Chem.*, 2008, **56**, 6717–6723.
21 Y. Houminer and S. Patai, *Tetrahedron Lett.*, 1967, 1297–1300.
22 J. B. Paine, Y. B. Pithawalla and J. D. Naworal, *J. Anal. Appl. Pyrolysis*, 2008, **83**, 37–63.
23 K. Kato, *Agric. Biol. Chem.*, 1967, **31**, 657–663; Y. Zhang, C. Liu and H. Xie, *J. Anal. Appl. Pyrolysis*, 2024, **105**, 23–34; M. Wang, C. Liu, X. Xu and Q. Li, *J. Anal. Appl. Pyrolysis*, 2016, **120**, 464–473; B. Hu, Q. Lu, X. Y. Jiang, X. C. Dong, M. S. Cui, C. Q. Dong and Y. P. Yang, *J. Energy Chem.*, 2018, **27**, 486–501; O. W. He, Y. F. Zhang, P. Wang, L. N. Liu, Q. Wang, N. Yang, W. J. Li, P. Champagne and H. B. Yu, *Catalysts*, 2021, **11**, 11–23.
24 K. Kato and H. Komorita, *Agric. Biol. Chem.*, 1968, **32**, 715–720; E. Anet, *J. Am. Chem. Soc.*, 1960, **82**, 1502; R. J. van Putten, J. C. van der Waal, E. de Jong, C. B. Rasrendra, H. J. Heeres and J. G. de Vries, *Chem. Rev.*, 2013, **113**, 1499–1597; A. Fukutome, H. Kawamoto and S. Saka, *ChemSusChem*, 2016, **9**, 703–712; M. R. Nimlos, S. J. Blanksby, X. H. Qian, M. E. Himmel and D. K. Johnson, *J. Phys. Chem. A*, 2006, **110**, 6145–6156; T. Honma and H. Inomata, *J. Supercrit. Fluids*, 2014, **90**, 1–7.
25 T. Nomura, E. Minami and H. Kawamoto, *RSC Adv.*, 2020, **10**, 7460–7467.
26 F. J. Kilzer and A. Broido, *Pyrodynamic*, 1965, **2**, 151–163; A. G. W. Bradbury, Y. Sakai and F. Shafizadeh, *J. Appl. Polym. Sci.*, 1979, **23**, 3271–3280.
27 S. Matsuoka, H. Kawamoto and S. Saka, *Carbohydr. Res.*, 2016, **420**, 46–50.
28 G. N. Richards, F. Shafizadeh and T. T. Stevenson, *Carbohydr. Res.*, 1983, **117**, 322–327.
29 H. Kawamoto, T. Hosoya, Y. Ueno, T. Shoji and S. Saka, *J. Anal. Appl. Pyrolysis*, 2014, **109**, 41–46.
30 M. Chidambaram and A. T. Bell, *Green Chem.*, 2010, **12**, 1253–1262.